Long- and Short-Range Interactions between Phospholipid/Ganglioside GM1 Bilayers†

Thomas J. McIntosh*,‡ and Sidney A. Simon§

Departments of Cell Biology, Neurobiology, and Anesthesiology, Duke University Medical Center, Durham, North Carolina 27710

Received April 27, 1994; Revised Manuscript Received June 21, 1994®

ABSTRACT: The structure and interactive properties of liquid–crystalline egg phosphatidylcholine (EPC) bilayers containing the ganglioside GM1 and its uncharged analogue, asialoGM1 (AGM1), have been obtained by X-ray diffraction analysis of osmotically stressed liposomes. Both electron density profiles and reciprocal space modeling indicate that (1) the incorporation of up to 30 mol % GM1 into EPC bilayers has little effect on bilayer organization and (2) the oligosaccharide portion of the GM1 molecule extends at least 12 Å beyond the EPC head group into the fluid space, implying that the GM1 head group is nearly fully extended from the bilayer surface. Pressure–distance relations for EPC:GM1 bilayers in 100 mM ionic strength buffer show that, for large bilayer separations, the interbilayer repulsive pressure decays exponentially with a decay length and magnitude expected for electrostatic repulsion arising from the charged GM1. However, at interbilayer separations of ≤30 Å for 7:3 and 8:2 EPC:GM1 and ≤22 Å for 9:1 EPC:GM1, the pressure–distance curves have distinct upward breaks, with the sharpness of this break depending strongly on the amount of GM1 in the bilayer. For 7:3 EPC:GM1 bilayers, the break is quite sharp so that the distance between bilayers does not decrease below 28 Å with further increases in applied pressure. For EPC:GM1 8:2 and 9:1 bilayers, the upward break becomes softer with decreasing GM1 concentration. For uncharged EPC:AGM1 bilayers, the repulsive pressure extends only to an equilibrium fluid separation of about 36 Å, but has a similar behavior to the pressure–distance data for EPC:GM1 for separations below 20 Å. We argue that the nonelectrostatic repulsive pressures arise primarily from the steric interactions between the hydrated oligosaccharide head groups that protrude from the bilayer surface.

Gangliosides are glycosphingolipids containing sialic acid that are found primarily in the outer surfaces of plasma membranes in every vertebrate tissue (Zeller & Marchase, 1992). They are most highly concentrated in neuronal and glial cells, where they comprise 5–10 mol % of the lipid in the plasma membrane (Derry & Wolfe, 1967). Since gangliosides are primarily located in the outer leaflet of the membrane, the external surfaces of some plasma membranes, such as those of glial cells, may contain from 10 to 20 mol % ganglioside. Gangliosides are thought to play roles in a number of cellular functions, including cell recognition and adhesion (Cheresh et al., 1984; Burns, 1988; Kojima & Hakomori, 1989; Hakomori, 1993), cell growth regulation (Yates et al., 1992), signal transduction (Hakomori, 1993), and development of tissues (Curatolo, 1987).

The ganglioside GM1,[1] which contains four neutral sugar residues and a negatively charged sialic acid residue (Figure 1), has been extensively investigated for several reasons. First, GM1 is a common ganglioside in many plasma membranes and can be incorporated into lipid bilayers to concentrations as high as 30 mol % GM1 (Hill & Lester, 1972; Bach et al., 1982). Second, GM1 is the receptor for the *Vibrio cholera* toxin B subunit (van Heyningen, 1974, 1982). Binding of this toxin to GM1 is the initial step in the induction of cholera. Third, when administered to animals, GM1 has been shown to accelerate neuronal regeneration and repair (Schengrund, 1990). Fourth, phospholipid bilayers containing GM1 are useful for modeling the electrostatic potentials adjacent to biological membranes (McDaniel et al., 1984; Beitinger et al., 1989; Luckham et al., 1993a). Fifth, GM1 can promote adhesion between planar lipid bilayers (Brewer & Thomas, 1986). Sixth, the incorporation of GM1 increases the blood circulation time of liposomes, providing a possible role for

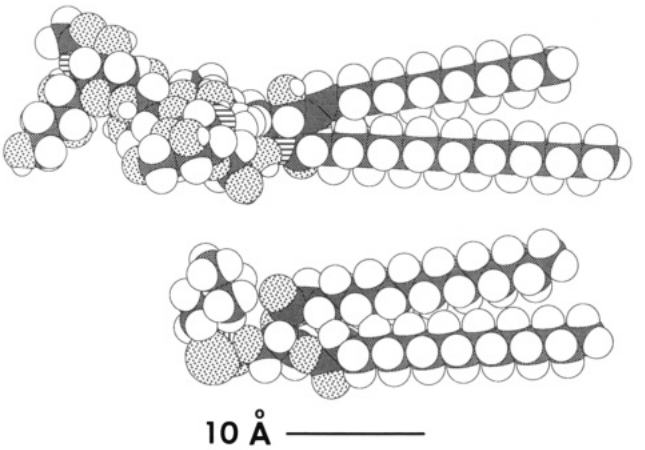

FIGURE 1: Space-filling models of GM1 (top) and phosphatidylcholine (PC) (bottom). In these models, hydrogen atoms are white, carbons are grey, oxygens are dotted, nitrogens have horizontal stripes, and the phosphorus of PC has vertical stripes. These models are presented simply to show the relative sizes of the GM1 and PC head groups. The depicted conformations of the lipid head groups are completely arbitrary.

† Supported by Grant GM-27278 from the National Institutes of Health.

‡ Department of Cell Biology.

§ Departments of Neurobiology and Anesthesiology.

® Abstract published in *Advance ACS Abstracts,* August 1, 1994.

[1] Abbreviations: GM1, galactosyl-*N*-acetylgalactosaminyl(*N*-acetylneuraminyl)galactosylglucosylceramide; AGM1, asialoGM1, galactosyl-*N*-acetylgalactosaminylgalactosylglucosylceramide; EPC, phosphatidylcholine derived from egg yolks; DPPC, dipalmitoylphosphatidylcholine; DOPC, dioleoylphosphatidylcholine; SOPC, 1-stearoyl-2-oleoylphosphatidylcholine.

0006-2960/94/0433-10477$04.50/0

GM1-containing liposomes in drug delivery (Allen & Chonn, 1987; Allen et al., 1989; Mori et al., 1991; Gabizon & Papahadjopoulos, 1992; Park & Huang, 1993).

To understand the role of GM1 in bilayers or membranes, it is important to determine the conformation of the GM1 head group and the effects that GM1 has on bilayer structure and interactive properties, including electrostatic, hydration, and steric pressures. With respect to these interactive properties, the increased circulation time provided by the incorporation of GM1 might depend on either the electrostatic or steric barrier produced by the GM1 molecule (Gabizon & Papahadjopoulos, 1992; Woodle & Lasic, 1992), and the observation that GM1 inhibits phospholipase activity has been interpreted in terms of a steric effect produced by the GM1 head group (Bianco et al., 1990). Quantitative information on GM1's effects on the nonspecific interactions between bilayers will also help define the role of this ganglioside in bilayer adhesion (Brewer & Thomas, 1986).

Previous studies have provided structural data on GM1 in bilayers. ESR measurements of GM1 in phospholipid bilayers and in membranes indicated that the oligosaccharide head group is both mobile and capable of forming intermolecular H-bonds (Sharom & Grant, 1978). NMR studies of GM1 in phosphatidylcholine micelles revealed that the terminal disaccharides are much more mobile than the branched core inner trisaccharide, where the sialic acid is stabilized in position by H-bonds (Acquotti et al., 1991). Other NMR measurements of GM1 micelles in DMSO/D_2O suggested that the sialic acid residue is oriented more toward the terminal galactose moiety and forms intramolecular H-bonds with the N-acetyl group on GalNAc (Scarsdale et al., 1990). X-ray diffraction studies on egg phosphatidylcholine (EPC) bilayers containing 0.3 mol fraction GM1 revealed that the GM1 head group extends at least 21 Å from the hydrocarbon–water interface (McDaniel & McIntosh, 1986).

The interactions between GM1 and GM1–phosphatidylcholine monolayers adsorbed to either mica surfaces or phosphatidylethanolamine monolayers bound to mica surfaces were investigated using a surface force apparatus (Parker, 1990; Luckham et al., 1993b). These studies found that, at large bilayer separations, the repulsive interactions could be modeled with classic electrostatic double-layer theory. However, at smaller bilayer separations, where deviations from double-layer interactions were observed, it was argued that the interactions were due to steric or hydration interactions between the GM1 head groups. Although the surface force apparatus is extremely useful for measuring pressure–distance relations and has the particular advantages that it can measure attractive interactions and interactions between apposing bilayers of different compositions, it is difficult with this apparatus to obtain quantitative pressure–distance relations for small bilayer separations (Marra & Israelachvili, 1985; Parker, 1990). Moreover, lipid layers bound to solid substrates are constrained and therefore do not display thermally induced undulations that give rise to repulsive pressures in free-standing membranes or bilayers (Harbich & Helfrich, 1984; Evans & Parsegian, 1986; Evans, 1991).

In this paper, we use X-ray diffraction to determine the structure of GM1 in EPC bilayers. We also use the osmotic stress technique (Parsegian et al., 1979; McIntosh & Simon, 1986b) to measure pressure–distance relationships between these bilayers, in particular determining the total repulsive pressure at small interbilayer separations. By comparing pressure–distance data from EPC bilayers containing various concentrations of the charged GM1 and the uncharged AGM1, we separate the contributions of electrostatic and steric pressures to the total interaction profile.

MATERIALS AND METHODS

EPC was obtained from Avanti Polar Lipids. Monosialoganglioside-G_{M1} from bovine brain (GM1), asialoganglioside-G_{M1} from bovine brain (AGM1), and poly(vinylpyrrolidone) (PVP) of average molecular weight 40 000 were obtained from Sigma Chemical Co.

Two types of lipid systems were examined by X-ray diffraction, unoriented suspensions of multiwalled vesicles and oriented multibilayers. Known osmotic pressures were applied to both of these systems by published procedures (LeNeveu et al., 1977; Parsegian et al., 1979; McIntosh & Simon, 1986a; McIntosh et al., 1987). To prepare both types of systems, EPC and the appropriate mole fractions of GM1 or AGM1 were first codissolved in chloroform. For the liposome preparation, the chloroform was removed by rotary evaporation. Osmotic stress was applied to EPC:GM1 or EPC:AGM1 liposomes by incubating the dry lipids for several hours in solutions of the neutral polymer PVP with periodic vortexing. It was shown that equilibrium was reached under these conditions, since longer incubation times (up to 3 days) did not change the X-ray diffraction patterns obtained from these specimens. PVP solutions in the range of 0–60% w/w were made in 100 mM ionic strength buffer (76 mM NaCl, 100 mM HEPES, at pH 7.0). Since PVP is too large to enter the lipid lattice, it competes for water with the lipid multilayers, thereby applying an osmotic pressure (LeNeveu et al., 1977). Osmotic pressures for the PVP solutions were calculated from the virial coefficients of Vink (1971). These values are in close agreement with values measured by McIntosh et al. (1989b). The lipid/PVP suspensions were sealed in quartz X-ray capillary tubes and mounted in a point-collimator X-ray camera.

Oriented EPC:GM1 and EPC:AGM1 multilayers were prepared by drying a drop of the appropriate chloroform solution onto a small piece of aluminum foil. The substrate was given a convex curvature by bending it around a Pasteur pipet as described previously (McIntosh et al., 1987). The multilayers on the aluminum substrate were mounted in a controlled humidity chamber on a single-mirror (line-focused) X-ray camera such that the X-ray beam was oriented at a grazing angle relative to the multilayers (McIntosh et al., 1987, 1989a). Pressures were applied to the oriented multibilayers by incubating them in constant relative humidity atmospheres maintained with saturated salt solutions. To speed equilibration, a gentle stream of nitrogen was passed through a flask of the saturated salt solution and then through the chamber. The ratio of the vapor pressure (p) of various salt solutions to the vapor pressure of pure water (p_o) has been determined (O'Brien, 1948; Weast, 1984). The applied pressure is given by

$$P = -(RT/V_w) \ln(p/p_o) \quad (1)$$

where R is the molar gas constant, T is the temperature in degrees kelvin, and V_w is the partial molar volume of water (Parsegian et al., 1979).

For both oriented and unoriented specimens, X-ray diffraction patterns were recorded at a temperature of 20 °C on Kodak DEF X-ray film. X-ray films were processed by standard techniques and densitometered with a Joyce-Loebl microdensitometer as described previously (McIntosh & Simon, 1986b; McIntosh et al., 1987). After background

subtraction, integrated intensities, $I(h)$, were obtained for each order, h, by measuring the area under each diffraction peak. For unoriented patterns, the structure amplitude $F(h)$ was set equal to $\{h^2I(h)\}^{1/2}$ (Blaurock & Worthington, 1966; Herbette et al., 1977). For the oriented line-focused patterns, the intensities were corrected by a single factor of h due to the cylindrical curvature of the multilayers (Blaurock & Worthington, 1966; Herbette et al., 1977) so that $F(h) = \{hI(h)\}^{1/2}$.

Electron density profiles, $\rho(x)$, on a relative electron density scale were calculated from

$$\rho(x) = (2/d)\sum \exp\{i\phi(h)\}\, F(h) \cos(2\pi xh/d) \qquad (2)$$

where x is the distance from the center of the bilayer, d is the lamellar repeat period, $\phi(h)$ is the phase angle for order h, and the sum is over h. Electron density profiles described in this paper are at a resolution of $d/2h_{max} \approx 6$ Å.

RESULTS

For oriented and unoriented EPC:GM1 and EPC:AGM1 specimens subjected to applied osmotic pressures, the X-ray diffraction patterns consisted of a series of low-angle reflections, which indexed as orders of a lamellar repeat period, and a broad wide-angle diffraction band centered at 4.5 Å. These patterns are characteristic of bilayers in the liquid–crystalline phase (Tardieu et al., 1973). In excess buffer with zero applied pressure, discrete lamellar reflections were recorded from EPC and EPC:AGM1 (see below). However, in excess buffer with zero applied pressure, no discrete X-ray reflections were recorded from EPC:GM1 bilayers containing 0.1–0.3 mol fraction of GM1, indicating that these bilayers swelled indefinitely in the absence of applied pressure.

The lamellar repeat period depended on both the mole fraction of GM1 or AGM1 in the bilayer and the applied osmotic pressure (Figure 2). Figure 2A shows a plot of the logarithm of applied pressure (log P) versus repeat period for EPC bilayers and EPC:GM1 bilayers at molar ratios of 7:3, 8:2, and 9:1 EPC:GM1 and Figure 2B shows a plot of log P versus repeat period for EPC and 8:2 EPC:GM1 and 8:2 EPC:AGM1 bilayers. For all of these plots, a single lamellar phase was recorded for each specimen at each applied pressure. For higher applied pressures (log $P > 8.3$), a second lamellar phase was also recorded, with a similar repeat period to that of pure EPC bilayers recorded at the same osmotic pressures. Since the EPC:GM1 molecular ratio is not known for the phase corresponding to larger repeat period in these phase separated samples, these data points are not shown in figure 2. Parker (1990) also observed that large pressures induced phase separation between dioleoylphosphatidylcholine and GM1 in experiments with the surface force apparatus.

For each bilayer composition, the lamellar repeat period decreased with increasing applied pressure (Figure 2). However, the shape of the pressure–distance relation was different for each system. First consider the two bilayers with no net charge, EPC and 8:2 EPC:AGM1 (Figure 2B). For pure EPC bilayers the lamellar repeat period was 63.2 Å at zero applied pressure (arrow marked E in Figure 2B) (McIntosh & Simon, 1986b) and decreased to a value of about 50 Å at an applied pressure of 3.2×10^8 dyn/cm^2 (log P = 8.5) (Figure 2B and (McIntosh et al., 1987)). For 8:2 EPC:AGM1 bilayers, the repeat period was 84.2 Å at zero applied pressure (arrow A in Figure 2B) and decreased to 67.9 Å at an applied pressure of 1.0×10^8 dyn/cm^2 (log P = 8.02). For all applied pressures, the repeat periods for 8:2 EPC:AGM1 were 15–20 Å larger than those of EPC. For bilayers

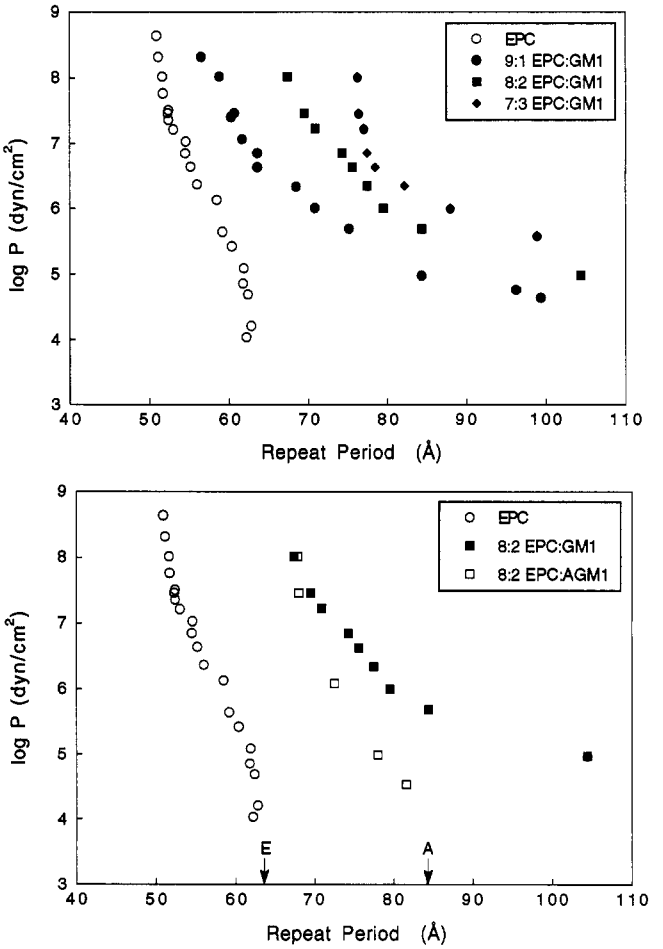

FIGURE 2: Logarithm of applied osmotic pressure plotted versus lamellar repeat period for (A, top) EPC bilayers (open circles), 9:1 EPC:GM1 bilayers (solid circles), 8:2 EPC:GM1 bilayers (solid squares), and 7:3 EPC:GM1 bilayers (diamonds) and (B, bottom) EPC bilayers (open circles), 8:2 EPC:GM1 bilayers (solid squares), and 8:2 EPC:AGM1 bilayers (open squares). In panel (B), the arrows labeled "E" and "A" mark the repeat periods obtained at zero applied pressures for EPC and 8:2 EPC:AGM1 bilayers, respectively. EPC data for log $P > 5.6$ are taken from the work of McIntosh and Simon (1986b) and McIntosh et al. (1987), and EPC data for log $P < 5.6$ are from Parsegian et al. (1979). Two types of lipid specimens were used in these experiments. The data points for log P = 7.5, 8.0, 8.3, and 8.5 were obtained from oriented specimens in controlled-humidity atmospheres, and all other data points were obtained from unoriented suspensions in PVP solutions.

containing GM1 (Figure 2A,B) no lamellar diffraction could be recorded in a 0.1 M ionic strength buffer in the absence of applied pressure, and at log P = 4.5, the repeat period was over 100 Å for all bilayers containing GM1 (Figure 2A). Specifically, for log $P < 7.5$, bilayers of 8:2 EPC:GM1 had larger repeat periods than bilayers of EPC:AGM1 8:2. Moreover, the pressure-distance relation depended strongly on the mole fraction of GM1 in the bilayer (Figure 2A).

To obtain information on the structure of the bilayers and the width of the fluid space between adjacent bilayers, a Fourier analysis was performed by procedures described previously (McIntosh & Simon, 1986b; McIntosh & Holloway, 1987). Figure 3 shows a plot of the structure factors versus reciprocal space coordinate for EPC and 9:1, 8:2, and 7:3 EPC:GM1 bilayers. All of the structure factors in this figure were from specimens where a single lamellar repeat period was observed. The diffraction data are plotted using the phase angles previously obtained for EPC bilayers (McIntosh & Simon, 1986b; McIntosh et al., 1987) and 7:3 1-stearoyl-2-oleoyl phosphatidylcholine:GM1 bilayers (McDaniel & McIntosh,

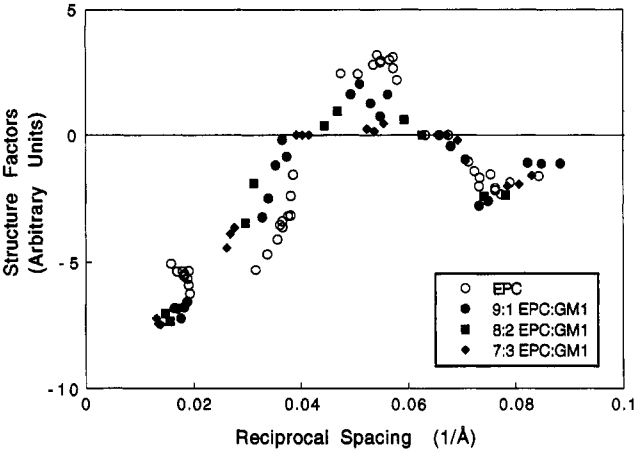

FIGURE 3: Structure factors plotted versus reciprocal space coordinates for EPC bilayers (open circles), 9:1 EPC:GM1 bilayers (solid circles), 8:2 EPC:GM1 bilayers (solid squares), and 7:3 EPC:GM1 bilayers (diamonds). Structure factors for EPC bilayers are from the work of McIntosh and Simon (1986b) and McIntosh et al. (1987).

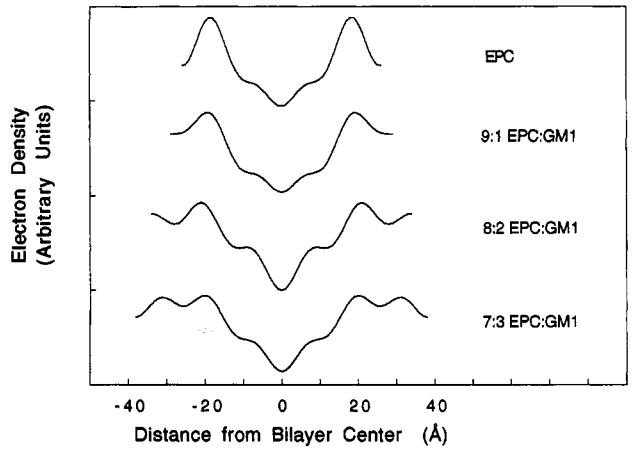

FIGURE 4: Electron density profiles of bilayers of EPC, 9:1 EPC:GM1, 8:2 EPC:GM1, and 7:3 EPC:GM1. All profiles were obtained at an applied osmotic pressure of $P = 1 \times 10^8$ dyn/cm^2.

1986). The following points should be noted about these observed structure factors. First, although the structure factors for the EPC bilayers containing GM1 were similar to those of pure EPC bilayers, there were significant differences, especially at the lower reciprocal spacings. For example, the first-order structure factors (between 0.016 and 0.020 Å^{-1}) were larger in magnitude for the bilayers containing GM1 than for EPC, whereas the second-order structure factors (between 0.025 and 0.038 Å^{-1}) were smaller in magnitude for the bilayers containing GM1 than for EPC (Figure 3). Second, the difference between the observed structure amplitudes for GM1-containing bilayers and EPC bilayers depended on the mole fraction of GM1. The largest differences in magnitude were observed between the structure amplitudes for EPC and 7:3 EPC:GM1.

Figure 4 shows electron density profiles for EPC bilayers and 7:3, 8:2, and 9:1 EPC:GM1 bilayers at the same applied pressure ($P = 1 \times 10^8$ dyn/cm^2, or log $P = 8$). For each profile, the geometric center of the bilayer is at the origin. The low electron density trough in the center of the bilayer corresponds to the localization of the terminal methyl groups of the lipid hydrocarbon chains, the medium density regions on each side of this trough correspond to the lipid methylene groups, the high density peaks centered near ±20 Å correspond to the phospholipid head groups, and the medium density regions outside the head group peaks correspond to the fluid spaces between adjacent bilayers. Several points should be noted from these profiles. First, the electron density distributions across the head group peak, methylene chain, and terminal methyl regions of the bilayer were similar in all four profiles. Second, the greatest change upon incorporation of GM1 occurred in the fluid space between bilayers. The incorporation of increasing amounts of GM1 increased both the width and the electron density of the fluid space between bilayers.

To determine more accurately the structural changes caused by the incorporation of GM1, we performed model calculations comparing the Fourier transforms of one-dimensional uniform electron density strip models to the observed X-ray data (Figure 5). Such strip models have have often been used in diffraction analysis of membranes and lipid bilayers (Worthington, 1969; Worthington & Blaurock, 1969; Franks et al., 1982; King et al., 1984; McDaniel & McIntosh, 1986; McIntosh & Holloway, 1987). The models for the EPC bilayer contained five uniform electron density strips corresponding to the terminal methyl region in the center of the bilayer, two methylene chain regions, and two phospholipid head group regions. The widths and absolute electron densities of each of the strips were similar to previous models used for similar lipids (McDaniel & McIntosh, 1986; McIntosh & Holloway, 1987). We used 47.8 Å for the total width of the EPC bilayer from our previous estimate for the bilayer width (McIntosh & Simon, 1986b). For the strips corresponding to the terminal methyl, methylene chain, and head group regions the densities were 0.27, 0.32, and 0.45 electrons/Å^3, respectively, and the widths were 8.0, 9.9, and 10.0 Å, respectively. (To simplify the calculations, a "minus fluid" model (Worthington et al., 1973) was used, whereby the electron density of the buffer, 0.336 electrons/Å^3, was subtracted from each of the strips. With this procedure the fluid space between bilayers had zero electron density and thus did not contribute to the Fourier transform.) For the bilayers containing GM1, we added two additional constant electron density strips on the outside of the bilayer corresponding to the carbohydrate moieties of GM1. We considered two models. In the first model, the widths and densities of the five strips in the bilayer were kept constant, and the densities and widths of the strips corresponding to the carbohydrate regions were varied until a good fit was obtained with the observed structure factors. For 9:1, 8:2, and 7:3 EPC:GM1 bilayers the electron densities for the carbohydrate regions were 0.367, 0.394, and 0.410 electrons/Å^3, respectively, and the widths of these regions were 11, 11, and 12 Å, respectively. These electron densities correspond to densities of concentrated sugar solutions. For comparison, a 1.0 M solution of galactose would have an electron density of about 0.39 electrons/Å^3. Including the width of the phospholipid bilayer and the extension of the GM1 head group, we calculate that the total thicknesses of the 9:1, 8:2, and 7:3 EPC:GM1 bilayers were 70, 70, and 72 Å, respectively. In the second model, both the width of the methylene chain region (in 0.5 Å increments) and the density of the head group region (in 0.01 electrons/Å^3 increments) were varied to determine if the bilayer structure was appreciably modified by the incorporation of GM1. A good fit to the data was obtained with the same strip widths as used for the EPC bilayers, showing that the bilayer structure did not markedly change upon the addition of GM1. A small improvement in the fit (see Figure 5A–C) was obtained by decreasing the density of the phospholipid head group region from 0.45 to 0.43 electrons/Å^3 for 7:3 EPC:GM1 and to 0.44 electrons/Å^3 for both 8:2 and 9:1 EPC:GM1. This decrease

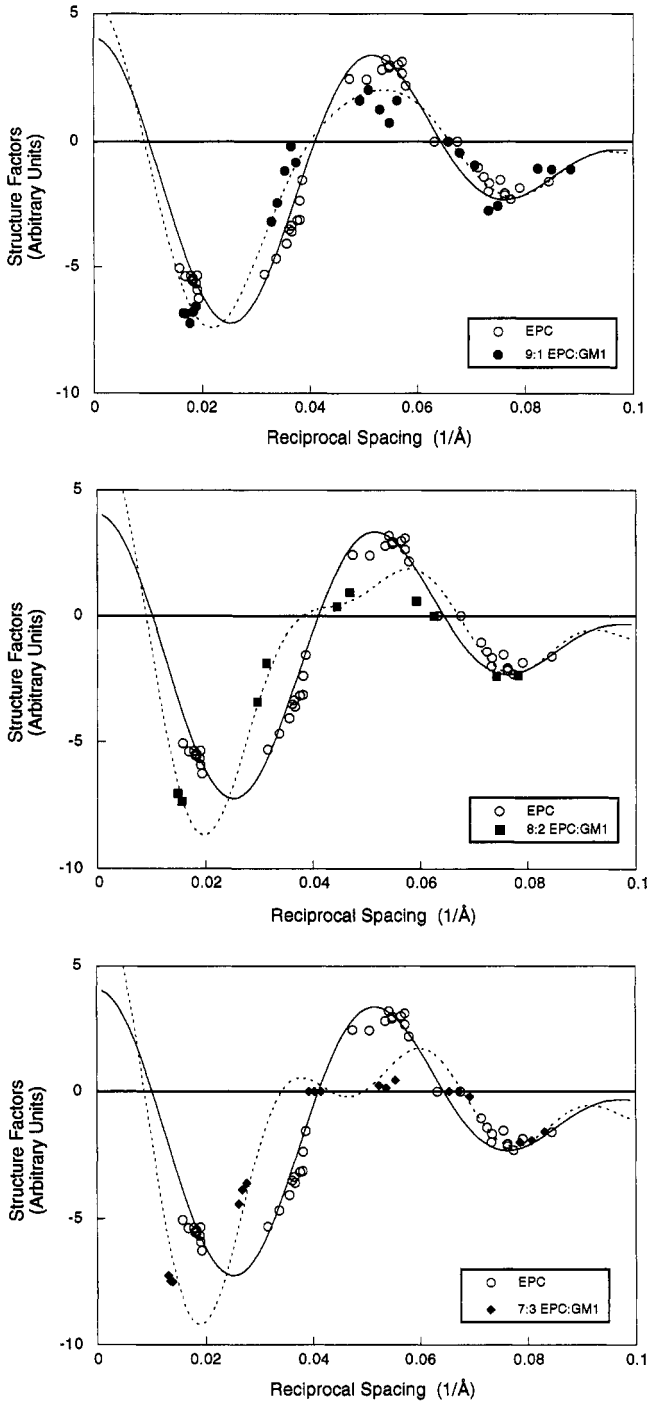

FIGURE 5: Structure factors plotted versus reciprocal space coordinate for (A, top) EPC bilayers (open circles) and 9:1 EPC:GM1 bilayers (solid circles), (B, middle) EPC bilayers (open circles) and 8:2 EPC:GM1 (solid squares), and (C, bottom) EPC bilayers (open circles) and 7:3 EPC:GM1 bilayers (diamonds). In each panel, the solid line represents the Fourier transform of a five-strip uniform electron density strip model of an EPC bilayer and the dotted line represents the transform of a seven-strip electron density model of EPC:GM1 bilayers that contains two additional constant electron density strips on the outside of the bilayer corresponding to the carbohydrate moieties of the GM1 molecules. For all bilayers, the widths of the terminal density, methylene chain, and head group regions of the bilayer were 8, 9.9, and 10.0 Å, respectively. For all bilayers the densities of the terminal methyl and methylene strips were 0.27 and 0.32 electron/Å^3, respectively. For EPC, 9:1 EPC:GM1, 8:2 EPC:GM1, and 7:3 EPC:GM1 bilayers the density of the head group strips were 0.45, 0.44, 0.44, and 0.43 electron/Å^3, respectively. For 9:1 EPC:GM1, 8:2 EPC:GM1, and 7:3 EPC:GM1 the electron densities for the carbohydrate regions were 0.367, 0.394, and 0.410 electrons/Å^3, respectively, and the widths of these regions were 11, 11, and 12 Å, respectively.

in density indicates that the portion of the GM1 molecule located in the head group region of the EPC bilayer had a smaller density than the EPC head group.

Thus, both the electron density profiles (Figure 4) and the model calculations (Figure 5) indicate that the incorporation of up to 0.3 mol fraction GM1 did not appreciably change the width or structure of the EPC bilayer.

These X-ray results can be used to estimate the distance between adjacent bilayer surfaces as a function of applied pressure. As noted previously (McIntosh & Simon, 1986b; McIntosh et al., 1987, 1989a), the definition of the edge of the bilayer is somewhat arbitrary, because the bilayer surface is not smooth and water penetrates into the head bgroup region of the bilayer (Worcester & Franks, 1976; Simon et al., 1982; Nagle & Wiener, 1988; Wiener et al., 1991). As a reference point, we used the outer edge of the EPC bilayer, so that we operationally defined the bilayer width (d_b) as the total thickness of the EPC bilayer with its head group parallel to the plane of the bilayer (McIntosh & Simon, 1986b; McIntosh et al., 1987, 1989a). This width of the EPC bilayer, according to our previous analysis for EPC and according to the model calculations (Figure 5), was 47.8 Å for EPC and EPC:GM1 bilayers. We assume that 8:2 EPC:AGM1 bilayers also had this same bilayer thickness. To be consistent with our previous work (McIntosh & Simon, 1986b, 1993, McIntosh et al., 1987, 1989a), the distance between the EPC bilayer surfaces (d_f) was calculated as the difference between the lamellar repeat period (d) and this EPC bilayer thickness (d_b).

Using this definition of the lipid/water interface, we plot in Figure 6A the common logarithm of applied pressure versus d_f for EPC and 7:3, 8:2, and 9:1 EPC:GM1 bilayers and in Figure 6B log P versus d_f for EPC, 8:2 EPC:GM1, and 8:2 EPC:AGM1 bilayers. The incorporation of GM1 to EPC increased the distance between the surfaces of adjacent EPC bilayers at all pressures (Figure 6A). With osmotic pressure applied, the relative increase in interbilayer space depended on the amount of GM1 incorporated into the bilayer. In particular, for each applied pressure the largest interbilayer spacings were recorded for 7:3 EPC:GM1. For these bilayers, the distance between EPC surfaces was increased to over 50 Å at an applied pressure of log P = 5.6 (Figure 6A). As the applied pressure was increased to log P = 6.6, the distance between bilayers decreased to about 30 Å. The plot of log P versus distance for 7:3 EPC:GM1 was nearly linear for interbilayer spaces of 35 Å < d_f < 50 Å, implying that for this range of d_f the repulsive pressure between bilayers decreased exponentially with increasing interbilayer separation. Increasing the pressure to log P = 7.5 reduced the fluid spacing to about 28 Å, whereupon further increases in pressure did not produce additional changes in the fluid spacing. The pressure–distance relations for 8:2 and 9:1 EPC:GM1 bilayers were different in several regards (Figure 6A). First, for d_f > 30 Å, the pressure–distance relations were shifted to smaller pressures with decreasing amounts of GM1 in the bilayers. Second, the slope of the upward break in the pressure–distance curve (observed at d_f = 30 Å for 7:3 EPC:GM1) decreased with decreasing GM1 concentration. At high applied pressures (log $P \geq 8$), the distance between bilayers was considerably smaller for 9:1 and 8:2 EPC:GM1 than for 7:3 EPC:GM1 (Figure 6A). For EPC:AGM1 8:2 bilayers, the maximum fluid spacing, which corresponds to the equilibrium fluid spacing at zero applied pressure, was 36 Å (arrow in Figure 6B), and log P versus d_f was approximately linear from d_f = 33 Å to d_f = 23 Å with a decay length of about 2.5 Å (linear fit not shown). For log P > 7.5, increasing the osmotic pressure

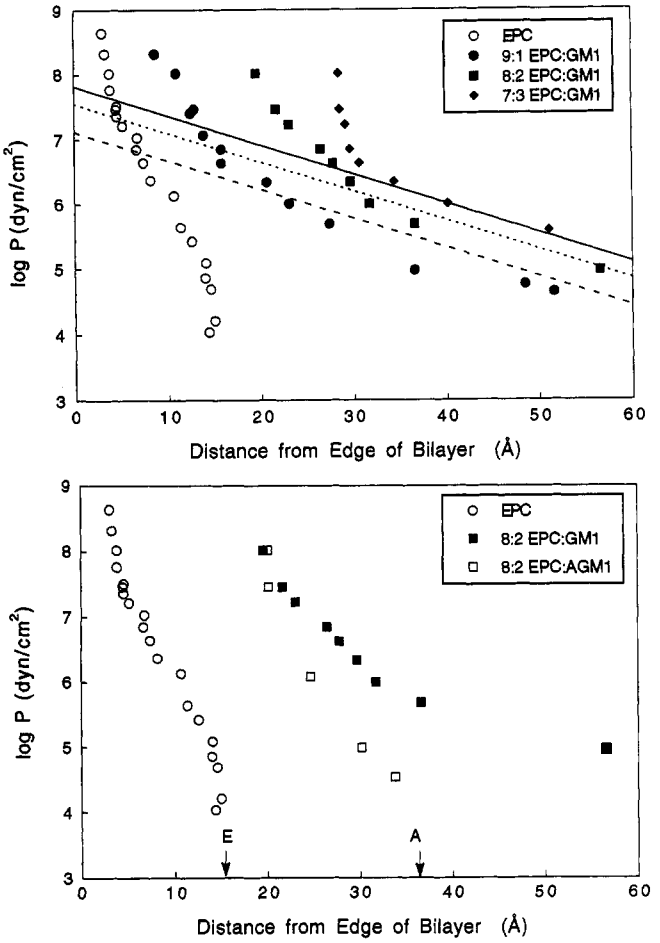

FIGURE 6: Logarithm of applied osmotic pressure plotted versus distance between the surface of the EPC bilayer for (A, top) EPC bilayers (open circles), 9:1 EPC:GM1 bilayers (solid circles), 8:2 EPC:GM1 bilayers (solid squares), and 7:3 EPC:GM1 bilayers (diamonds) and (B, bottom) EPC bilayers (open circles), 8:2 EPC:GM1 bilayers (solid squares), and 8:2 EPC:AGM1 bilayers (open squares). Distance data for EPC bilayers for log $P > 5.6$ were taken from the work of McIntosh and Simon, (1986b) and McIntosh et al. (1987) and EPC data for log $P < 5.6$ were calculated from the repeat period data of Parsegian et al. (1979) (Figure 2) by subtracting a constant bilayer thickness of 47.8 Å, as described in the text. In panel A, the dashed, dotted, and solid lines are calculations from electrostatic double-layer theory for the electrostatic pressure between 9:1 EPC:GM1 bilayers, 8:2 EPC:GM1 bilayers, and 7:3 EPC:GM1 bilayers, respectively (see the text for details). In panel B, the arrows labeled "E" and "A" mark the fluid spaces obtained at zero applied pressures for EPC and 8:2 EPC:GM1 bilayers, respectively.

did not result in a further reduction of d_f. 8:2 EPC:GM1 bilayers had much larger fluid spacings at low pressures than 8:2 EPC:AGM1 bilayers, but had approximately the same fluid spacings for log $P > 6.5$ (Figure 6B).

DISCUSSION

The data presented in this paper provide information on (1) the structural changes in the phosphatidylcholine bilayer caused by the incorporation of various concentration of ganglioside GM1, (2) the location of GM1 in the bilayer, and (3) the effects of GM1 and AGM1 on interbilayer pressures.

Structure of EPC/GM1 Bilayers. Both the electron density profiles (Figure 4) and reciprocal space modeling analysis (Figure 5) indicate that up to 0.3 mol fraction GM1 can be incorporated into liquid–crystalline EPC bilayers without appreciably changing its structure. Specifically, the shape of the hydrocarbon region and the distance between the head group peaks across the bilayer are similar for EPC bilayers and 7:3, 8:2, and 9:1 EPC GM1 bilayers (Figure 4). These analyses show that the major effect of GM1 on the electron density profiles is to increase the interbilayer distance between the EPC head groups and to add electron density to the fluid space between bilayers. At high applied pressures (log $P \approx 8$), both the width and electron density of the fluid space increase with increasing concentrations of GM1 (Figure 4). The modeling analysis shows the same effects and, in addition, provides a quantitative estimate of the bilayer width and width and electron density of the fluid space as a function of GM1 concentration. In particular, this analysis shows that GM1 has no detectable effect on bilayer thickness and causes only a small decrease in the electron density of the lipid head group region. This reduction in electron density of the polar head group suggests that part of the GM1 head group is intercalated between EPC head groups since the electron density of the carbohydrate moieties of GM1 is smaller than the electron density of the PC head group. The modeling studies provide more accurate information on the effects of GM1 on bilayer thickness than the electron density profiles, since the addition of the relatively electron dense carbohydrate groups in the fluid space between bilayers tends to shift outward the head group peaks in the profiles. Although electron density profiles for 8:2 EPC:AGM1 bilayers were not constructed due to the limited resolution of the diffraction data, we assume that incorporation of this lipid into EPC bilayers also does not alter the structure of EPC.

Location of GM1 in Bilayer. The most reasonable interpretation of these structural data is that the hydrocarbon chains of GM1 incorporate fully into the EPC bilayer so that their incorporation does not appreciably modify the structure of the bilayer's hydrocarbon interior. To minimize the large (50 erg/cm²) energetic cost of exposing hydrocarbon to water (Tanford, 1980; Israelachvili, 1991), the hydrocarbon/water interface for the ceramide and glycerol backbones should be approximately coplanar. The increased density in the fluid layer in the GM1 containing bilayer is evidence that the GM1 head group extends into the interbilayer fluid space at least 12 Å beyond the edge of the EPC head group (assuming that the EPC head group is oriented approximately parallel to the bilayer surface), or about 22 Å from the hydrocarbon/head group interface. This result is in excellent agreement with the extension of the GM1 head group into the fluid space for 7:3 SOPC:GM1 bilayers calculated by McDaniel and McIntosh (1986). The length of the fully extended GM1 head group from the ceramide backbone to its outer edge as measured by using a CPK model is about 22 Å (McDaniel et al., 1984). Since the width of the PC polar head group is about 10 Å (McIntosh & Simon, 1986b), the value of 12 Å obtained from the model calculations for 7:3 EPC:GM1 bilayers is consistent with a model in which the glucose attached to the ceramide backbone is intercalated between the PC head groups with the remainder of the oligosaccharide extending approximately perpendicularly into the fluid space.

Effect of GM1 Incorporation on Interbilayer Pressures. The incorporation of GM1 into EPC bilayers has two major effects on the observed pressure–distance relations (Figure 6). First, at low applied pressures (log $P < 6$), GM1 causes large increases in the interbilayer fluid space. Second, for high applied pressures (log $P > 6$), the incorporation of between 0.1 and 0.3 mol fraction GM1 produces upward breaks in the pressure–distance relations such that the interbilayer space is always larger in the bilayer containing GM1. The sharpness of this upward break increases with increasing GM1 concentration (Figure 6A). We consider the effects of GM1 on

the pressure–distance relations in terms of the various pressures that can occur between adjacent bilayers, namely the repulsive electrostatic, hydration, and steric pressures and the attractive van der Waals pressure.

We first consider the low-pressure region ($\log P < 6$). For this region, two pieces of evidence indicate that the large increases in interbilayer spacing caused by incorporation of GM1 must be primarily due to the electrostatic repulsion arising from the surface charge produced by the sialic acid of the GM1 molecule, as argued previously by Parker (1990) and Luckham et al. (1993b). First, for $\log P < 6$ the lamellar repeat period for EPC:GM1 is considerably larger than the repeat period for EPC containing comparable amounts of the uncharged AGM1 (Figure 2B). Second, the magnitude and decay length of the pressures for EPC:GM1 bilayers in this region can be accounted for by classical double layer theory. The electrostatic repulsive pressure between two planar, charged surfaces at constant surface potential is given by

$$P_{es} = (64kT)c\gamma^2 \exp(-KD) \quad (3)$$

where T is temperature, c is the bulk electrolyte concentration, $\gamma = \tanh(e\psi_o/4kT)$ where ψ_o represents the membrane surface potential, K is the Debye length, and D is the distance between the planes where the charges are located (Israelachvili, 1991). For 100 mM 1:1 electrolytes $K = 1/(9.6\ \text{Å})$ and ψ_o can be evaluated from the Gouy–Chapman equation, $\sinh(\psi_o/51.4\ \text{mV}) = 136\sigma/(c)^{1/2}$, where σ is the surface charge density (in electrons/Å^2). To calculate σ, we use an area per molecule of 64 Å^2 for EPC and 100 Å^2 for GM1, values consistent with X-ray diffraction analysis of EPC (McIntosh et al., 1989b; McIntosh & Simon, 1986b) and monolayer studies of GM1 (Maggio et al., 1978). We also assume that all GM1 molecules in the bilayer are charged, since the pK_a of sialic acid is 2.6. We equate D with our value of d_f, since McDaniel et al. (1986) found that their electrokinetic data for PC/GM1 bilayers could be explained with the charge of GM1 located 10 Å from the hydrocarbon/water interface, or precisely at our choice of $d_f = 0$. Using these values and assumptions, we use eq 3 to calculate the expected electrostatic repulsive pressure for 7:3, 8:2, and 9:1 EPC:GM1 bilayers. These theoretical predictions are shown as the straight lines in Figure 6A. For 7:3, 8:2, and 9:1 EPC:GM1 bilayers the theoretical predictions are quite close to the experimental data points for $d_f \geq 35$, 32, and 24 Å, respectively.

We now consider the pressure–distance data for interbilayer spacings smaller than these values, where the experimental data points deviate from the predictions of electrostatic theory (Figure 6A). For the following reasons we argue that the differences in the pressure–distance relations for EPC and EPC:GM1 bilayers for $\log P > 6$ must be primarily due to steric interactions caused by the relatively bulky GM1 head group (Figure 1). First, at least for $\log P > 7$, the relative contribution of electrostatics must be small, since 8:2 EPC:GM1 and 8:2 EPC:AGM1 have similar pressure–distance relations for $\log P > 7$ (Figure 6B). Second, the upward break at $d_f \approx 30$ Å for 7:3 EPC:GM1 is much too sharp to be explained solely by relatively "soft" interactions such as the hydration pressure (LeNeveu et al., 1977; Parsegian et al., 1979; McIntosh & Simon, 1986b), the undulation pressure (Harbich & Helfrich, 1984; Evans & Parsegian, 1986; Evans, 1991), or the protrusion pressure (Israelachvili & Wennerstrom, 1990, 1992). Third, as discussed in detail below, the range of the pressure for 7:3 EPC:GM1 bilayers for $\log P > 6$ can be explained primarily in terms of the extension of the GM1 head group into the fluid space between bilayers. Fourth, as also detailed below, the observation that the sharpness of the upward break depends on the amount of GM1 incorporated into the bilayer (Figure 6A) is consistent with a steric hindrance (or excluded volume) interaction between GM1 head groups. That is, higher surface densities of GM1 would tend to cause stiffer steric barriers and sharper upward breaks in the pressure–distance relations (Figure 6A). In this regard, the pressure–fluid spacing interactions between EPC:GM1 bilayers (Figure 6A) resemble those obtained for bilayers containing different concentrations of lipids with covalently bound short polymers (Kuhl et al., 1994).

We now consider the third point listed above, the position of the upward break in the pressure distance relation for 7:3 EPC:GM1 bilayers. The electron density profiles (Figure 4) and reciprocal space modeling studies show for these bilayers that the carbohydrate moiety extends into the fluid space between adjacent bilayers, at least 12 Å from the edge of the EPC bilayer. Thus, the modeling predicts that GM1 molecules from apposing bilayers should come into direct molecular contact at $d_f \geq 24$ Å. For 7:3 EPC:GM1, as the applied pressure is increased, the pressure–d_f curve (Figure 6A) has an upward break that starts at about 33 Å and reaches a minimum value of $d_f \approx 28$ Å before phase separation occurs. The difference in position of the predicted "hard wall" repulsion at 24 Å, due to molecular contact, and the observed upward break in the pressure–distance relation from 33 to 28 Å (Figure 6A) can be rationalized by several factors. First, our strip model analysis assumes a sharp cutoff for the outward projection of the GM1 head group at a strip width of 12 Å. The outer edge of GM1 head groups obviously do no form a perfectly smooth boundary, and the molecules may actually extend more than 12 Å from the edge of the EPC head group. Second, the lipid membrane is fluid and thermally induced bilayer undulations (Harbich & Helfrich, 1984; Evans & Parsegian, 1986; Evans, 1991) and head group motions are undoubtedly present. Such motions would tend to extend the range of the steric interaction caused by the GM1 head groups. In addition, binding of water to the hydrophilic GM1 head group may also extend the range of the steric barrier. A single layer of water bound to the GM1 molecules could increase the effective extension of the GM1 molecule about 3 Å from each bilayer. In other words, the approximately 4–9 Å difference in range of the steric pressure from predicted hard core steric interactions to the observed upward breaks in the pressure–distance relation (Figure 6A) could arise from the presence of bilayer undulations, relaxation of the configurational entropy of the polar head group, and the adsorption of waters of hydration.

The primary differences in the nonelectrostatic repulsive interactions between 7:3 and 8:2 EPC:GM1 bilayers are for $\log P > 7$, where for 7:3 EPC:GM1 bilayers d_f remained nearly constant with increasing pressure, whereas for 8:2 EPC:GM1 bilayers d_f decreased with increasing pressure (Figure 6A). There are two models that are consistent with the presence of the softer upward break in the pressure–distance curve for 8:2 EPC:GM1 at high applied pressures: (1) partial interpenetration of GM1 head groups from apposing bilayers and (2) change in the conformation of the GM1 head group. We consider each possibility in turn. If one assumes that the area per EPC molecule is 64 Å^2 (McIntosh et al., 1989b) and the area per molecule of a GM1 molecules is about 100 Å^2 (Maggio et al., 1978), then in a 7:3 EPC:GM1 bilayer about 40% of the surface area is covered by GM1, whereas in the 8:2 EPC:GM1 bilayer only about 28% of the surface is covered by GM1. Thus, there is a greater likelihood of interpenetration

of apposing GM1 head groups in the case of 8:2 EPC:GM1. Previously we had noted upward breaks in the pressure–distance relations for EPC (McIntosh et al., 1987, 1989a; McIntosh & Simon, 1994) and sphingomyelin bilayers (McIntosh et al., 1992), which we argued were due to steric repulsion between head groups from apposing bilayers. In the case of EPC, there was a similar dependence to that shown in Figure 6A on the surface concentration of EPC head groups. That is, as the surface concentration of EPC was reduced by the addition of spacer molecules such as cholesterol, the sharpness of the upward break decreased, until no break was observed when the area per EPC head group was such that head groups from apposing bilayers could interpenetrate (McIntosh et al., 1989a). Relative to the second possibility, it has been shown by NMR that the mobile external disaccharides (Galβ1-4Glc) of the GM1 head group exist in several conformations (Acquotti et al., 1991). At a lower surface coverage (8:2), where lateral interactions between the GM1 molecules are weaker than in 7:3 bilayers, it is possible at high applied pressures ($\log P > 7$) that steric interactions from apposing bilayers could force the GM1 head groups from one conformation to another. A conformational change of about 35° in the terminal Galβ1 moiety (Stokes diameter ≈ 7 Å), from a more perpendicular to a more planar orientation, would decrease the fluid thickness a total of approximately 8 Å to $d_f \approx 16$ Å, which is approximately the thickness of two monosaccharides.

For 9:1 EPC:GM1 bilayers, the upward deviation from the electrostatic pressure is quite gradual (Figure 6A) and, at an applied pressure of $\log P = 8$, the fluid space decreases to about 9 Å. In other words, the fluid space has attained the dimensions close to that of a single monosaccharide, suggesting that, at low GM1 concentrations, the GM1 head groups have both interdigitated and squeezed into a coplanar configuration by the apposing PC bilayer. Thus, at the highest applied pressures, the spacing between 7:3 EPC:GM1 bilayers is limited by saccharide–saccharide interactions whereas for the 9:1 EPC:GM1 bilayers the spacing is probably limited by saccharide–EPC interactions.

In summary, the nonelectrostatic work to reduce the fluid spacing between EPC:GM1 bilayers arises primarily from the work to compress the saccharides and the work to increase the concentration of osmotically active material in the interlamellar spacing. The range of the pressure is related to the extension of the head group, and the pressure–distance relations indicate that the GM1 head group must be nearly fully extended perpendicular to the bilayer surface, at least in the case of 7:3 and 8:2 EPC:GM1 bilayers.

The results of previous surface force apparatus measurements (Parker, 1990; Luckham et al., 1993b) of the interactions between PC:GM1 membranes coated on mica surfaces are similar to our results in two ways: (1) there is a long-range electrostatic interaction between membranes predicted by double-layer theory and (2) there are upward breaks in the pressure–distance relations ascribed to steric/hydration interactions. However, the positions of the upward breaks in the surface force measurements are more difficult to interpret on a molecular level than our X-ray results, since the X-ray analysis (Figures 3–5) provides direct information on the bilayer structure, whereas the surface force measurements do not. For instance, in one series of surface force measurements by Parker (1990), 9:1 DOPC:GM1 of 9:1 DPPC:GM1 monolayers were transferred to mica surfaces previously coated with hydrophobic surfaces formed from monolayers of dimethyldioctadecylammonium bromide/dipalmitoylphosphatidylethanolamine. For 9:1 DOPC:GM1 and 9:1 DPPC:GM1, the upward breaks were observed at separations of the hydrophobic surfaces of about 45 and 90 Å, respectively (Parker, 1990). These distances should be equivalent to the X-ray repeat periods, since they should contain the thickness of two monolayers plus the intermonolayer fluid space. Considering that the thickness of a gel phaseDPPC bilayer is about 5 Å larger than a liquid crystalline EPC bilayer (McIntosh & Simon, 1986b), the 9:1 DPPC:GM1 surface force apparatus results are not too different than our X-ray results (Figure 2A). However, the upward break at 45 Å for 9:1 DOPC:GM1 is inconsistent with our data (Figure 2A), since 45 Å is smaller even than the thickness of a bare EPC (or DOPC) bilayer. Parker (1990) argues that there are two possible explanations for "this smaller than expected bilayer thickness": (1) the GM1 head group might "fold down" and (2) the contact region might be depleted of gangliosides due to lateral diffusion as the surfaces are brought together. Luckham et al. (1993b) used 3:1 DPPC:GM1 bilayers transferred directly onto mica surfaces by the Langmuir–Blodgett dipping methods. They found an upward break in the pressure–distance relations at a distance from the mica surfaces of 186 Å. This distance presumably corresponds to the thickness of two bilayers plus the fluid space between bilayers. In the case of 7:3 EPC:GM1 bilayers, we find the equivalent spacing to be 174 Å (2 times the total bilayer thickness = 2·72 Å = 144 Å, plus $d_f \approx 30$ Å). Again considering that the bilayer thickness of DPPC is about 5 Å larger than the bilayer thickness of EPC (McIntosh & Simon, 1986b), the results of Luckham et al. (1993b) and ours are very similar for the position of the steric barrier.

Range of Steric Pressures for AGM1 Bilayers. We next consider the interactions between 8:2 EPC:AGM1 bilayers. The advantage of investigating uncharged AGM1 bilayers, compared with GM1 bilayers, is that the pressure–distance relation (Figure 6B) does not contain the contributions of electrostatic repulsion. This means that the nonelectrostatic part of the interaction can be measured to lower applied pressures (Figure 6B), and additional information can be obtained on the effects of gangliosides on the magnitude of the attractive van der Waals pressure.

The interactions between the two electrically neutral bilayers, EPC and 8:2 EPC:AGM1, have approximately parallel pressure–distance relations but are displaced from each other by a thickness of about 16–20 Å (Figure 6B). For EPC bilayers the pressure–distance relation has been interpreted in terms of the attractive van der Waals pressure (LeNeveu et al., 1977) and several nonspecific repulsive pressures, including the hydration pressure from partially oriented water molecules (Marcelja & Radic, 1976; LeNeveu et al., 1977; McIntosh et al., 1989b; McIntosh & Simon, 1986b; Rand & Parsegian, 1989), the undulation pressure from thermally driven undulations in the bilayer (Harbich & Helfrich, 1984; Evans & Parsegian, 1986), a protrusion pressure from lipid molecules extending from the bilayer surface (Israelachvili & Wennerstrom, 1990, 1992), and a steric pressure from interactions between the mobile head groups from apposing bilayers (McIntosh et al., 1987, 1989a). We argue that, because of the nearly parallel nature of the pressure–distance relations for EPC and 8:2 EPC:AGM1, the same types of pressures may be present between 8:2 EPC:AGM1 bilayers. As argued above for 8:2 EPC:GM1 bilayers, the larger separation for EPC:AGM1 bilayers compared to EPC bilayers is undoubtedly due to the longer range steric

pressures due to the larger size of the AGM1 head group compared to the EPC head group.

At zero applied pressure the separation between AGM1 bilayers is about 36 Å (arrow marked "A" in Figure 6B). At this equilibrium fluid spacing the net repulsive pressure must be balanced by the van der Waals pressure, providing us with information on this attractive pressure. Since 8:2 EPC:AGM1 bilayers have an equilibrium fluid spacing about 20 Å larger than that of EPC bilayers (arrows Figure 6B), and since the attractive van der Waals energy (E_v) is proportional to H/d_f^2, where H is the Hamaker constant, it follows that at the equilibrium fluid spacing the van der Waals energy between the hydrocarbon regions of the bilayers must be greatly reduced for EPC:AGM1 compared to EPC. In fact, assuming that the Hamaker constant between the hydrocarbon regions of the bilayer is the same for EPC and 8:2 EPC:AGM1 bilayers, then the magnitude of the van der Waals energy between 8:2 EPC:GM1 bilayers at d_f = 36 Å would be reduced to 18% of its value at 15 Å. This would not be of sufficient magnitude to provide a stable adhesion energy (Evans & Parsegian, 1986). Thus, since 8:2 EPC:AGM1 bilayers do not swell indefinitely in excess water, we consider the possibility that the Hamaker constant increased with the addition of AGM1. It has been shown both theoretically (Nir, 1976) and experimentally (Evans & Needham, 1987) that the presence of saccharides in the head group region can increase the interactions between bilayers by increasing the van der Waals interactions between the aqueous phase and the polar head group phase. For lipid bilayers, the Hamaker constant (H) can be expressed as the sum of terms having the following functional forms (LeNeveu et al., 1977): $\sum(\epsilon_a - \epsilon_p/\epsilon_a + \epsilon_p)^2$, $\sum(\epsilon_a - \epsilon_p)/\epsilon_a + \epsilon_p)$ $(\epsilon_h - \epsilon_p/\epsilon_h + \epsilon_p)$, and $\sum(\epsilon_h - \epsilon_p/\epsilon_h + \epsilon_p)^2$, where ϵ_a is the dielectric susceptibility of the aqueous phase, ϵ_p is the dielectric susceptibility of the polar head group region, ϵ_h is the dielectric susceptibility of the hydrocarbon phase, and $\sum$ represents the sum over all frequencies. The dispersion for the polar head groups is not known (Attard et al., 1988), and thus cannot be accurately quantified. However, since carbohydrates have a higher polarizability than water, and our reciprocal space analysis shows that the fluid spaces for 7:3, 8:2, and 9:1 EPC:GM1 bilayers contain high concentrations of the GM1 head groups, the major contribution to the increase in H must come predominantly from the term $\sum(\epsilon_a - \epsilon_p/\epsilon_a + \epsilon_p)^2$. An independent estimate of an upper bound of the Hamaker constant can be obtained by noting that 8:2 EPC:GM1 bilayers swell indefinitely (Figure 6A), meaning that in that case the electrostatic energy is greater than the adhesion energy. For 1:1 electrolytes the repulsive double layer energy can be expressed as

$$E_{es} = (64kT)c\gamma^2/K \exp(-KD) \quad (4)$$

where the terms were described previously. For 8:2 EPC:GM1 bilayers, ψ_o = −53 mV, giving E_{es} = 0.56 erg/cm^2 at d_f = 17.5 Å. Since E_{es} is greater than the attractive energy for 8:2 EPC:GM1 bilayers, and if the attractive energy is assumed to arise from the van der Waals energy, it follows that $H > 2.6 \times 10^{-12}$ erg. This value of H is too large to be attributable to van der Waals interactions between layers of hydrocarbons, where $H \approx 5 \times 10^{-14}$ ergs (Israelachvili, 1991). This suggests that 8:2 EPC:AGM1 bilayers, like digalactosyl diacylglycerol bilayers (Evans & Needham, 1987), are stabilized by van der Waals interactions between the polarizable saccharides and the water phase.

Possible Biological Significance. From these studies several conclusions can be drawn that may be relevant to the role of GM1 in biological membranes. First, for EPC:GM1 bilayers the successful application of double layer theory to explain the long-range interactions suggests that GM1 molecules, in the absence of exogenously added Ca^{2+}, are uniformly distributed in the plane of the bilayer. Second, the interactions of EPC:GM1 bilayers are repulsive and thus (in the absence of exogenously added Ca^{2+}) cannot promote adhesion with like molecules. Third, the indication that the Hamaker constant, and thus the attractive van der Waals pressure, is increased by the presence of the oligosaccharides is significant since glycolipids have been shown to be involved in various processes involving adhesion (Hakomori, 1993). Fourth, since the glucose linked to the ceramide in GM1 is intercalated in the polar head group in PC bilayers, it is not likely to be recognized as an antigenic site. Fifth, for cells in which the plasma membrane GM1 concentration is 10 mol % (implying that the outer monolayer contains 20 mol % GM1), the GM1 head groups must be nearly fully extended and may form a significant steric barrier for large hydrophilic molecules to penetrate the cell membrane.

REFERENCES

Acquotti, D., Fronza, G., Ragg, E., & Sonnino, S. (1991) *Chem. Phys. Lipids 59*, 107–125.

Allen, T. M., & Chonn, A. (1987) *FEBS Lett. 223*, 42.

Allen, T. M., Hansen, C., & Rutledge, J. (1989) *Biochim. Biophys. Acta 981*, 27–35.

Attard, P., Mitchell, D. J., & Ninham, B. W. (1988) *Biophys. J. 53*, 457–460.

Bach, D., Miller, I. R., & Sela, B. (1982) *Biochim. Biophys. Acta 686*, 233–239.

Beitinger, H., Vogel, V., Mobius, D., & Rahmann, H. (1989) *Biochim. Biophys. Acta 984*, 293–300.

Bianco, I. D., Fidelio, G. D., & Maggio, B. (1990) *Biochim. Biophys. Acta 1026*, 179–185.

Blaurock, A. E., & Worthington, C. R. (1966) *Biophys. J. 6*, 305–312.

Brewer, G. J., & Thomas, P. D. (1986) *Neurochem. Res. 11*, 1321–1331.

Burns, G. F. (1988) *J. Cell Biol. 107*, 1225–1230.

Cheresh, D. A., Harper, J. R., Schulz, G., & Reisfeld, R. A. (1984) *Proc. Natl. Acad. Sci. U.S.A. 81*, 5767–5771.

Curatolo, W. (1987) *Biochim. Biophys. Acta 906*, 137–160.

Derry, D. M., & Wolfe, L. S. (1967) *Science 158*, 1450–1452.

Evans, E. (1991) *Langmuir 7*, 1900–1908.

Evans, E., & Needham, D. (1987) *J. Phys. Chem. 91*, 4219–4228.

Evans, E. A., & Parsegian, V. A. (1986) *Proc. Natl. Acad. Sci. U.S.A. 83*, 7132–7136.

Franks, N. P., Melchior, V., Kirshner, D. A., & Caspar, D. L. D. (1982) *J. Mol. Biol. 155*, 133–153.

Gabizon, A., & Papahadjopoulos, D. (1992) *Biochim. Biophys. Acta 1103*, 94–100.

Hakomori, S.-i. (1993) *Biochem. Soc. Trans.* 583–595.

Harbich, W., & Helfrich, W. (1984) *Chem. Phys. Lipids 36*, 39–63.

Herbette, L., Marquardt, J., Scarpa, A., & Blasie, J. K. (1977) *Biophys. J. 20*, 245–272.

Hill, M. W., & Lester, R. (1972) *Biochim. Biophys. Acta 282*, 18–30.

Israelachvili, J. N. (1991) *Intermolecular and Surface Forces*, pp 231–249, Academic Press, London.

Israelachvili, J. N., & Wennerstrom, H. (1990) *Langmuir 6*, 873–876.

Israelachvili, J. N., & Wennerstrom, H. (1992) *J. Phys. Chem. 96*, 520–531.

King, G. I., Chao, N. M., & White, S. H. (1984) in *Neutrons in Biology* (Schoenborn, B., Ed.) pp 159–172, Plenum Press, New York.

Kojima, N., & Hakomori, S.-i. (1989) *J. Biol. Chem. 264*, 20159–20162.
Kuhl, T. L., Leckband, D. E., Lasic, D. D., & Israelachvili, J. N. (1994) *Biophys. J. 66*, 1479–1488.
LeNeveu, D. M., Rand, R. P., Parsegian, V. A., & Gingell, D. (1977) *Biophys. J. 18*, 209–230.
Luckham, P., Wood, J., Froggatt, S., & Swart, R. (1993a) *J. Colloid Interface Sci. 156*, 164–172.
Luckham, P., Wood, J., & Swart, R. (1993b) *J. Colloid Interface Sci. 156*, 173–183.
Maggio, B., Cumar, F. A., & Caputto, R. (1978) *Biochemistry 171*, 559–578.
Marcelja, S., & Radic, N. (1976) *Chem. Phys. Lett. 42*, 129–130.
Marra, J., & Israelachvili, J. (1985) *Biochemistry 24*, 4608–4618.
McDaniel, R. V., & McIntosh, T. J. (1986) *Biophys. J. 49*, 94–96.
McDaniel, R. V., McLaughlin, A., Winiski, A., Eisenberg, M., & McLaughlin, S. (1984) *Biochemistry 23*, 4618–4623.
McDaniel, R. V., Sharp, K., Brooks, D., McLaughlin, A. C., Winiski, A. P., Cafiso, D., & McLaughlin, S. (1986) *Biophys. J. 49*, 741–752.
McIntosh, T. J., & Holloway, P. W. (1987) *Biochemistry 26*, 1783–1788.
McIntosh, T. J., & Simon, S. A. (1986a) *Biochemistry 25*, 4948–4952.
McIntosh, T. J., & Simon, S. A. (1986b) *Biochemistry 25*, 4058–4066.
McIntosh, T. J., & Simon, S. A. (1993) *Biochemistry 32*, 8374–8384.
McIntosh, T. J. & Simon, S. A. (1994) *Annu. Rev. Biophys. Biomol. Struct. 23*, 27–51.
McIntosh, T. J., Magid, A. D., & Simon, S. A. (1987) *Biochemistry 26*, 7325–7332.
McIntosh, T. J., Magid, A. D., & Simon, S. A. (1989a) *Biochemistry 28*, 17–25.
McIntosh, T. J., Magid, A. D., & Simon, S. A. (1989b) *Biochemistry 28*, 7904–7912.
McIntosh, T. J., Simon, S. A., Needham, D., & Huang, C.-h. (1992) *Biochemistry 31*, 2020–2024.
Mori, A., Klibanov, A. L., Torchilin, V. P., & Huang, L. (1991) *FEBS 284*, 263–266.
Nagle, J. F., & Wiener, M. C. (1988) *Biochim. Biophys. Acta 942*, 1–10.
Nir, S. (1976) *Prog. Surface Sci. 8*, 1–58.
O'Brien, F. E. M. (1948) *J. Sci. Instrum. 25*, 73–76.
Park, Y. S., & Huang, L. (1993) *Biochim. Biophys. Acta 1166*, 105–114.
Parker, J. L. (1990) *J. Colloid Interface Sci. 137*, 571–576.
Parsegian, V. A., Fuller, N., & Rand, R. P. (1979) *Proc. Natl. Acad. Sci. U.S.A. 76*, 2750–2754.
Rand, R. P., & Parsegian, V. A. (1989) *Biochim. Biophys. Acta 988*, 351–376.
Rau, D. C., & Parsegian, V. A. (1990) *Science 249*, 1278–1281.
Scarsdale, J. N., Prestegard, J. H., & Yu, R. K. (1990) *Biochemistry 29*, 9843–9855.
Schengrund, C.-L. (1990) *Brain Res. Bull. 24*, 131–141.
Sharom, F. J., & Grant, C. W. M. (1978) *Biochim. Biophys. Acta 507*, 280–293.
Simon, S. A., McIntosh, T. J., & Latorre, R. (1982) *Science 216*, 65–67.
Tanford, C. (1980) *The Hydrophobic Effect*, 2nd ed., Wiley, New York.
Tardieu, A., Luzzati, V., & Reman, F. C. (1973) *J. Mol. Biol. 75*, 711–733.
van Heyningen, S. (1974) *Science 183*, 656–657.
van Heyningen, S. (1982) in *Molecular Action of Toxins and Viruses* (Cohen, P., & van Heyningen, S., Eds.) pp 169–190, Elsevier, New York.
Vink, H. (1971) *Eur. Polym. J7*, 1411–1419.
Weast, R. C. (1984) *Handbook of Chemistry and Physics*, CRC Press, Boca Raton, FL.
Wiener, M. C., King, G. I., & White, S. H. (1991) *Biophys. J. 60*, 568–576.
Woodle, M. C., & Lasic, D. D. (1992) *Biochim. Biophys. Acta 1113*, 171–199.
Worcester, D. L., & Franks, N. P. (1976) *J. Mol. Biol. 100*, 359–378.
Worthington, C. R. (1969) *Biophys. J. 9*, 222–234.
Worthington, C. R., & Blaurock, A. E. (1969) *Biophys. J. 9*, 970–990.
Worthington, C. R., King, G. I., & McIntosh, T. J. (1973) *Biophys. J. 13*, 480–494.
Yates, A. J., Agudelo, J. D., & Sung, C.-C. (1992) *Lipids 27*, 308–310.
Zeller, C. B., & Marchase, R. B. (1992) *Am. J. Physiol. 262*, C1341–C1355.